

# Speckle-Tracking Imaging at the Australian Synchrotron

## Preliminary results from speckle-tracking studies at IMBL

Sheridan Mayo<sup>1</sup>, Konstantin Pavlov<sup>2</sup>, David Paganin<sup>3</sup>, Josh Bowden<sup>4</sup>, Thomas Li<sup>2</sup>, Marcus Kitchen<sup>3</sup>, Anton Maksimenko<sup>5</sup>, Ben Kennedy<sup>2</sup>, Andrew Stevenson<sup>5</sup>

1. CSIRO, Clayton, VIC, 2. University of Canterbury, Christchurch, New Zealand, 3. Monash University, Clayton, VIC, 4. CSIRO IMT, St Lucia, QLD, 5. Australian Synchrotron, Clayton, VIC

Speckle-tracking is one of a number of related imaging methods enabling the independent extraction of absorption, phase and dark-field images of a sample. Here we outline first results using this method at IMBL.

### Speckle-tracking Introduction

Speckle-tracking imaging utilises highly structured illumination created using a random mask such as sandpaper, and imaged with a detector placed at a suitable distance. The presence of a sample modifies the image of the mask, and by analysing the local changes in the intensity, visibility and position of the mask features, the absorption, refraction and dark-field images of the sample can be extracted.

To improve resolution, multiple image-pairs with and without the sample are collected, with the mask in a different position for each pair. Algorithms such as XVST<sup>1</sup>, and UMPA<sup>2</sup> are used to analyse the data.

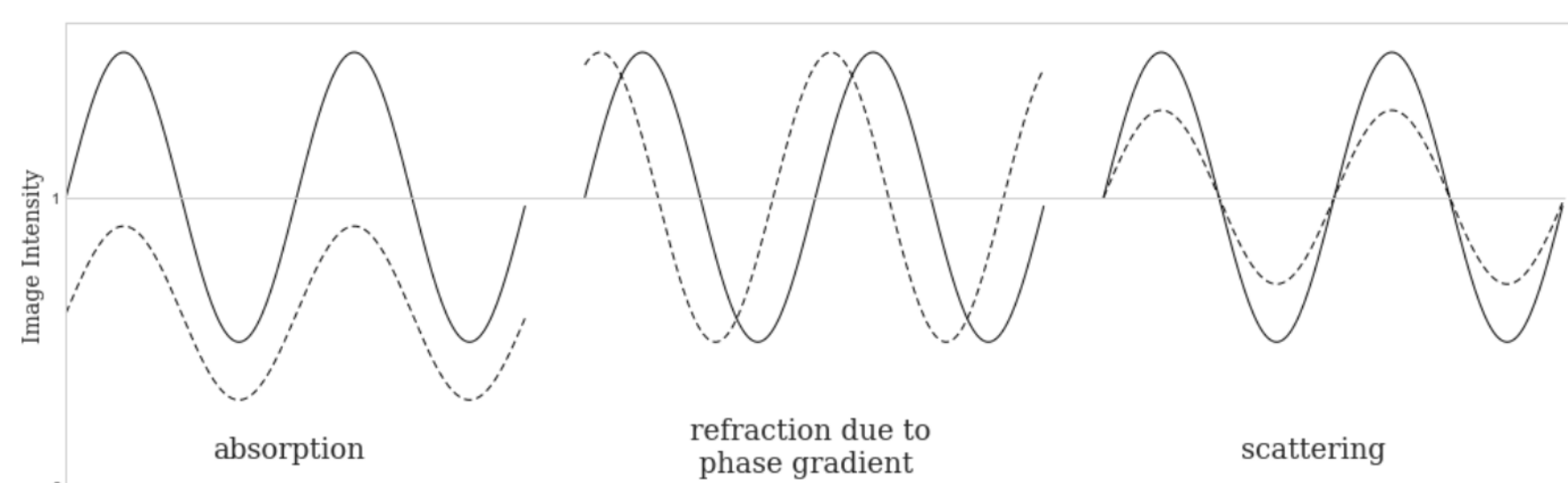


Figure 1: Sketch showing how a line-profile of intensity modulations from the mask is affected by different characteristics of the sample

### Test imaging and improved XVST software

For imaging we used two masks composed of 10 payers of P240 and P400 grit sandpaper respectively which had speckles of around 30-50 microns in size. A test sample was prepared composed of 1mm diameter nylon fibres, a 3 mm diameter graphite rod and two thin sheets of wood oriented at 90 degrees to one another. The mask and test sample were placed on the sample stage and imaging was carried out with the detector placed at distances of 1m, 2m and 4m from the sample. At each distance 25 image pairs were collected with the mask moved to different positions at least 150 microns apart.

Data were analysed using an improved version of XVST code developed during Josh Bowden's visit to ESRF. Images were successfully extracted (Fig. 2) showing different resolution and noise characteristics depending on the imaging distance and mask feature size (Fig. 3) and the size of the subarea used to analyse each point in the image (Fig. 4).

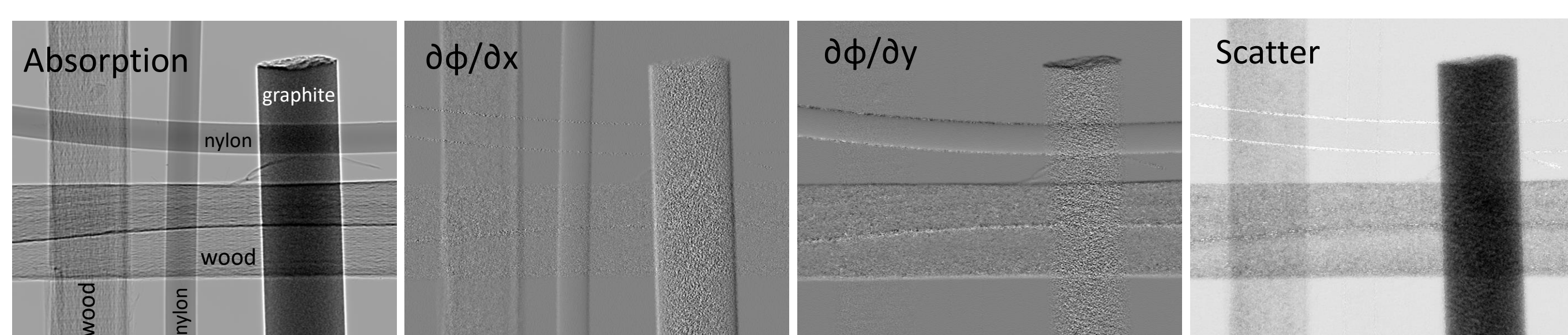


Figure 2: Absorption, phase gradient (in x and y) and scatter signal images extracted for images acquired at 1m using XVST

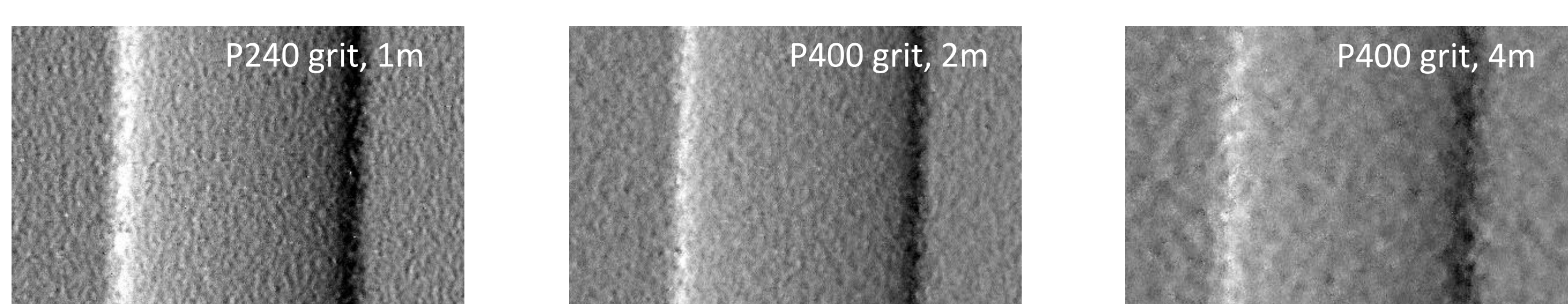


Figure 3: Detail of phase gradient in X from XVST analysis using 11x11 pixel subarea with different imaging distances and grit sizes. In general larger distances reduces spatial resolution (compare 2m and 4m images) whereas a finer grit (P400) improves resolution so that 2m/P400 grit image is sharper than 1m/P240 grit image despite greater distance.

### Simple scatter signal extraction

Relative to the in-line phase-contrast method, the dark-field or scattering signal is the most valuable feature that speckle-tracking provides. We have trialled simple 'one-shot' methods for extracting this signal at modest resolution using images of the sample with ( $I_{M&S}$ ) and without ( $I_S$ ) the mask plus a reference mask image ( $I_M$ ). The mask-plus-sample image, is divided by the image of the sample on its own,  $I_{M&S}/I_S$ , to give  $I_N$  thus removing absorption effects from the image but leaving scatter effects. Compensating for speckle shifts due to sample refraction was also possible but found not to be necessary for this data due to the very small (subpixel) displacements.

The effect of sample scattering on a subregion of the mask image (A) is approximated by blurring of the corresponding region on the reference mask image (A'), where the magnitude of blurring corresponds to the scatter signal. The blurring was modelled in two ways :

1: **Laplacian method** – fit for C to give best match such that,

$$A(I_M) + C \times \nabla^2(A(I_M)) \approx A'(I_N)$$

2: **Asymmetric 2D Gaussian kernel convolution** (fit for  $\sigma_{maj}$ ,  $\sigma_{min}$ , and  $\Theta$ )

$A(I_M) * \text{Gaussian2D}(\sigma) \approx A'(I_N)$ , where \* represents convolution – see Fig.4

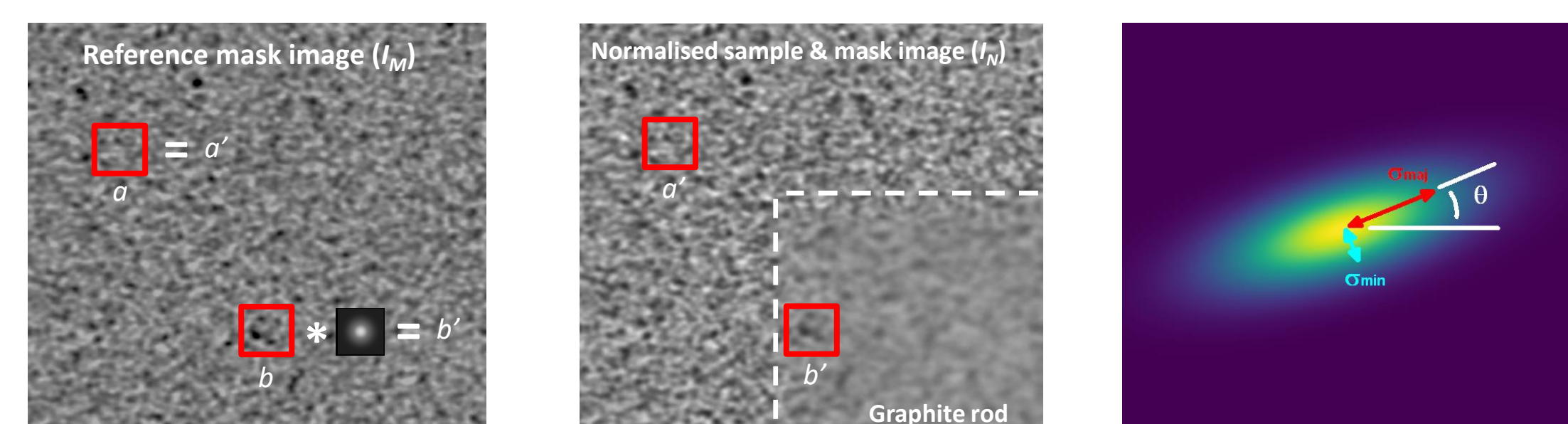


Figure 4: The normalised sample-plus-mask image shows scatter (blurring) at  $b'$  due to the graphite rod. The size of the blurring kernel which gives the best match between  $b * \text{Gaussian2D}(\sigma)$  and  $b'$  indicates the scattering strength. For directional blurring an asymmetric kernel was used with 3 parameters to fit;  $\sigma_{maj}$ ,  $\sigma_{min}$ , and  $\Theta$ .

The first method determines a uniform scattering signal at each subregion, while the second is sensitive to scattering asymmetry and orientation as is clearly demonstrated for the wood specimens (Fig. 5).

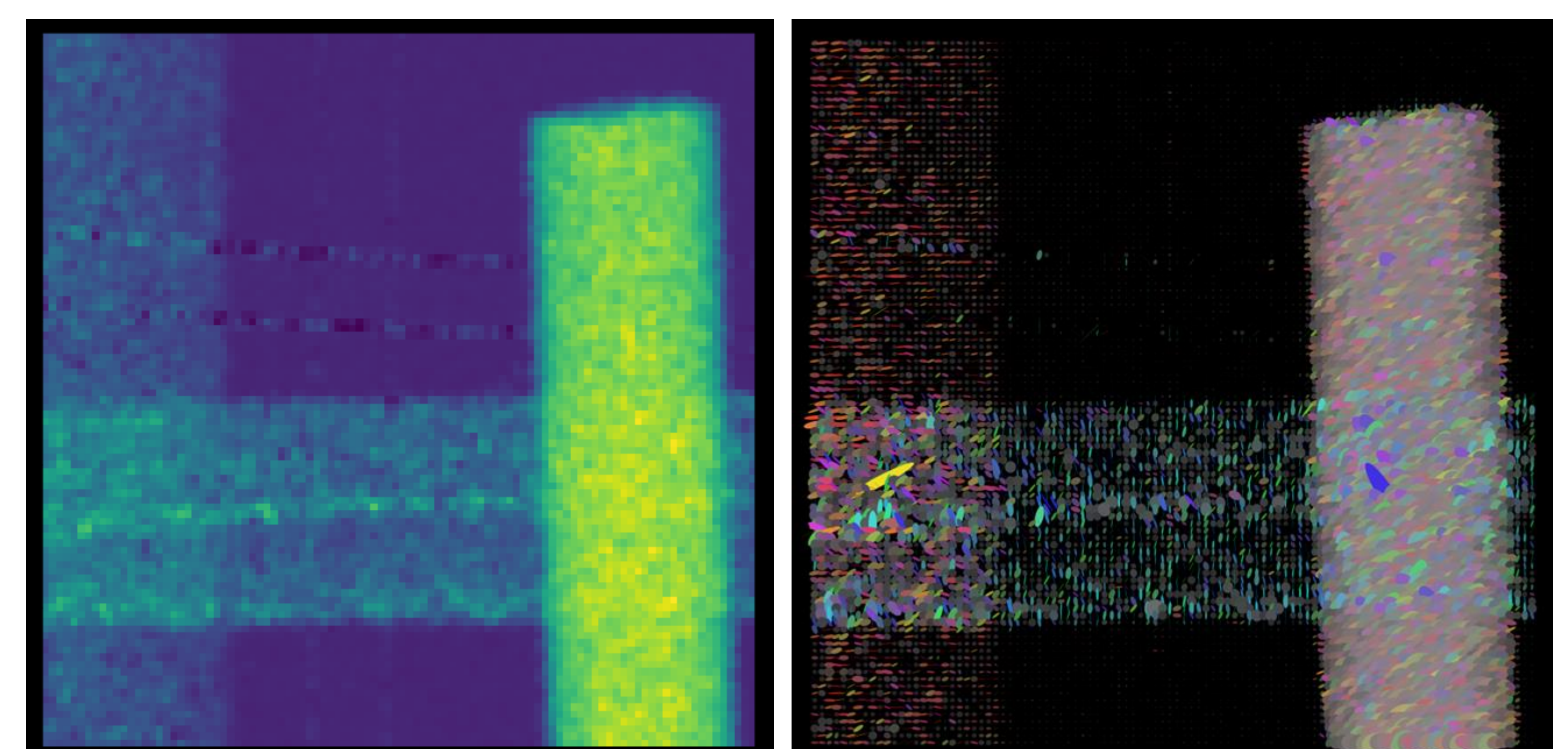


Figure 5: Left: uniform scatter determined from Laplacian approximation showing scatter for wood and graphite but not the nylon fibres. Right: asymmetric scatter at each point represented by ellipses with major, minor axes and orientation corresponding to  $\sigma_{maj}$ ,  $\sigma_{min}$ , and  $\Theta$  of the blurring kernel. Angle is also indicated by hue and asymmetry by saturation (grey = symmetric). The different orientation of the wood samples is clearly observed, with scattering perpendicular to fibres, whereas graphite scattering is strong but symmetric.